

CodeEnhance: A Codebook-Driven Approach for Low-Light Image Enhancement

Xu Wu, XianXu Hou, Zhihui Lai*, Jie Zhou, Ya-nan Zhang, Witold Pedrycz, Linlin Shen

Abstract—Low-light image enhancement (LLIE) aims to improve low-illumination images. However, existing methods face two challenges: (1) uncertainty in restoration from diverse brightness degradations; (2) loss of texture and color information caused by noise suppression and light enhancement. In this paper, we propose a novel enhancement approach, CodeEnhance, by leveraging quantized priors and image refinement to address these challenges. In particular, we reframe LLIE as learning an image-to-code mapping from low-light images to discrete codebook, which has been learned from high-quality images. To enhance this process, a Semantic Embedding Module (SEM) is introduced to integrate semantic information with low-level features, and a Codebook Shift (CS) mechanism, designed to adapt the pre-learned codebook to better suit the distinct characteristics of our low-light dataset. Additionally, we present an Interactive Feature Transformation (IFT) module to refine texture and color information during image reconstruction, allowing for interactive enhancement based on user preferences. Extensive experiments on both real-world and synthetic benchmarks demonstrate that the incorporation of prior knowledge and controllable information transfer significantly enhances LLIE performance in terms of quality and fidelity. The proposed CodeEnhance exhibits superior robustness to various degradations, including uneven illumination, noise, and color distortion.

Index Terms—Low-Light Image Enhancement, Codebook Learning, Vector-Quantized GAN.

I. INTRODUCTION

SUFFERING from low illumination intensity, diverse light sources, and color distortion issues, Low-Light (LL) images usually hinder visual perception and degrade the performance of downstream tasks [5]. To address these issues, the LLIE methods are proposed to obtain High-Quality (HQ) images from LL images [6].

This work was supported in part by the Natural Science Foundation of China under Grants 61976145, 61976144, 62076164, and 62272319, and in part by the Natural Science Foundation of Guangdong Province Grant 2314050002242, 2023A1515010677 and the Shenzhen Science and Technology Program under Grants JCYJ20210324094601005, JCYJ20210324094413037, and JCYJ20220818095803007. Corresponding author: Zhihui Lai

X. Wu, Z. Lai, Ya-nan Zhang and L. Shen are with the Computer Vision Institute, College of Computer Science and Software Engineering, Shenzhen University, Shenzhen 518060, China, Shenzhen Institute of Artificial Intelligence and Robotics for Society, Shenzhen 518060, China, and Guangdong Key Laboratory of Intelligent Information Processing, Shenzhen University, Shenzhen 518060, China (e-mail: csxunwu@gmail.com, lai_zhi_hui@163.com; zyn962464@gmail.com; llshen@szu.edu.cn).

X. Hou is School of AI and Advanced Computing, Xi'an Jiaotong-Liverpool University, China (hxianxu@gmail.com).

J. Zhou is National Engineering Laboratory for Big Data System Computing Technology, Shenzhen University, and SZU Branch, Shenzhen Institute of Artificial Intelligence and Robotics for Society, Shenzhen, Guangdong 518060, China (e-mail: jie_jpu@163.com).

W. Pedrycz is the Department of Electrical & Computer Engineering, University of Alberta, University of Alberta, Canada (wpedrycz@ualberta.ca).

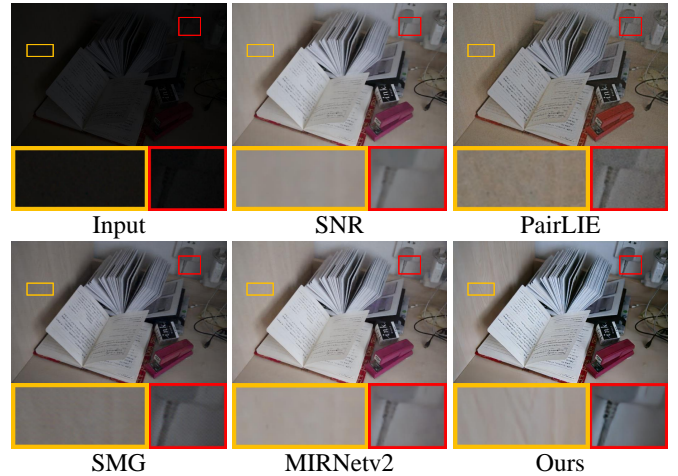


Fig. 1. Visual comparison on the LOL [1] dataset. It can be found that the proposed CodeEnhance outperforms other methods (SNR [2], SMG [3], and MIRNetv2 [4]) in terms of light enhancement, texture maintenance, noise suppression, and color restoration.

Classic LLIE methods based on histogram equalization [7] and retinex theories [8] [9], are effective in enhancing image brightness. However, these methods neglect image content and color, resulting in a distortion of the output image. Recently, deep learning-based methods [10] [11] have been leveraged due to their powerful expressiveness. The popular methods are mainly based on adversarial training [12] [13] or image-to-image [14] [15] framework, both of which aim to learn the mapping between LL and HQ images. Nevertheless, existing deep learning-based methods encounter limited generalization in real night scenes that contain complex light sources and the intricate illumination. Concretely, (1) The inherent uncertainty in the restoration process stems from addressing diverse brightness degradations, posing a considerable challenge to accurate reconstruction. (2) The loss of texture and color information arises due to the intricate balance required in simultaneous noise suppression and light enhancement, adding complexity to the image enhancement task.

To overcome these challenges, we propose a novel approach named CodeEnhance by feature matching with quantized priors and image refinement. Previous methods usually learn an LL-HQ image mapping, which typically involves a vast parameter space that brings uncertainty for the learning [16]. The key to reducing the uncertainty is to shrink the parameter space. Therefore, we reframe the LLIE task as an **image-to-code** paradigm by predicting the codebook indices, followed by the pretrained decoder to generate the output. This approach efficiently reduces the parameter space, which

alleviates uncertainties in the restoration process and improves robustness against various brightness degradations. Besides, we use the shallow features and introduce reference HQ images to compensate for the texture and color information in the output images, respectively. The rich texture information in shallow features [17] is used to assist the reconstruction. Moreover, the reference images provide valuable guidance for enhancing visual perception in the output.

Specifically, we develop a Semantic Embedding Module (SEM) to integrate semantic information and low-level features in the encoder of CodeEnhance. The SEM plays a crucial role in bridging the semantic gap and ensures effective feature alignment between the encoder and the codebook. Moreover, to address distribution shifts across datasets, we introduce a Codebook Shift (CS) mechanism. This mechanism is designed to adapt the pre-learned codebook from one dataset to better suit the distinct characteristics of our LLIE dataset, ensuring distribution consistency and emphasizing the relevant prior in feature matching. To enhance the restoration of texture and color, we design an Interactive Feature Transformation (IFT) module to fine-tune the texture, color, and brightness of the output image. The IFT consists of two main components: Texture Feature Transformation (TFT) module and Controllable Perceptual Transformation (CPT) module. The TFT module utilizes low-level features from the encoder to refine the details, and the CPT module leverages information from reference images to supplement color information and provide a reference standard for controllable enhancement. By incorporating these modules, we enable a step-by-step refinement process that improves the texture, color, and brightness of the restored image. This design also allows users to adjust the enhancement according to their visual perception, leading to improved customization and user satisfaction.

In summary, CodeEnhance mainly includes two stages. In Stage I, a VQ-GAN [18] is trained using HQ images. In Stage II, we utilize the HQ encoder, the SEM, and the CS to map the LL image to the codebook space. The matched codes are then fed into the frozen HQ decoder and the IFT to generate the enhanced image. Our contributions are listed as follows:

- We propose CodeEnhance, an innovative LLIE approach that employs a codebook, derived from high-quality images, as prior knowledge. This enables the transformation of low-light images into high-quality ones.
- To improve feature matching within the codebook, we introduce the Semantic Embedding Module (SEM) and the Codebook Shift (CS). These components enhance the consistency between the codebook and features learned by the encoder. Additionally, we design an Interactive Feature Transformation (IFT) module to enrich texture information in the decoder.
- Extensive experiments demonstrate that our proposed method achieves state-of-the-art performance on various benchmarks, including LOL, FiveK, and LSRW.

II. RELATED WORK

A. Low-Light Image Enhancement

Images captured in low-light environments often lack important visual details and exhibit poor image quality [19]. These

types of images can negatively impact the viewer’s experience and hinder their comprehension of the image content for further analysis. To address this issue, early researchers explored histogram equalization technology [7], which involves adjusting the illumination and contrast of the image by equalizing pixel intensity. They devised various LLIE methods that focused on the overall image perspective [20], cumulative function [21], and penalty terms [22]. In addition, there are many methods based on Retinex theory [9], which decomposes the image into two components: illumination and image reflection [8] [23]. With the advancements in deep learning technology, LLNet [6] has successfully integrated it into the field of LLIE for the first time by utilizing stacked autoencoders. To further improve image quality, multi-branch [24], and multi-stage [25] LLIE networks are developed, considering illumination recovery, noise suppression, and color refinement. SCI [26] uses a unique network structure in the training phase, where multiple stages share weights. However, during testing, only one sub-network is used. SNR [2] employs the PSNR distribution map of the image to guide network feature learning and fusion. SMG [3] incorporates image structure information to enhance the output image’s quality. Moreover, by combining Retinex theory with deep learning, URetinexNet [27] formulates the decomposition problem of Retinex as an implicit prior regularization model. Retinexformer [28] uses illumination to guide the Transformer [29] to learn the global illumination information of the image. However, these LLIE methods rely on LL image information for enhancement. This reliance makes them vulnerable to uncertain factors like noise and light sources, causing image artifacts, loss of details, and color distortion. To address these challenges, we propose a novel model that leverages high-quality prior knowledge to enhance its robustness against such uncertain factors. And a new feature transformation module is introduced to enable the algorithm to better handle variations in the input image.

B. Discrete Codebook Learning

Discrete codebook learning was initially introduced in the VQ-VAE [30]. After that, VQ-GAN [18] incorporates codebook learning into the GAN framework, enabling the generation of high-quality images. In low-level tasks, codebook learning is employed to mitigate uncertainty during the model learning process by transforming the operational space from the image into compact proxy space [16]. To improve feature matching, FeMaSR [31] introduces residual shortcut connections, RIDCP [32] proposes a controllable feature matching operation, and CodeFormer [16] presents a Transformer-based prediction network to obtain the codebook index, respectively. Moreover, LARSR [33] proposes a local autoregressive super-resolution framework based on the learned codebook. VQFR [34] designs parallel decoders to fuse low-level features from the encoder. Building upon the research above, our approach aims to redefine the low-light image enhancement task by introducing the codebook priors and learning the mapping between images and codebook indexes. Additionally, we propose a CS mechanism to fine-tune the original priors. This makes the priors better suitable for different datasets and enables our method to handle various illumination intensities.

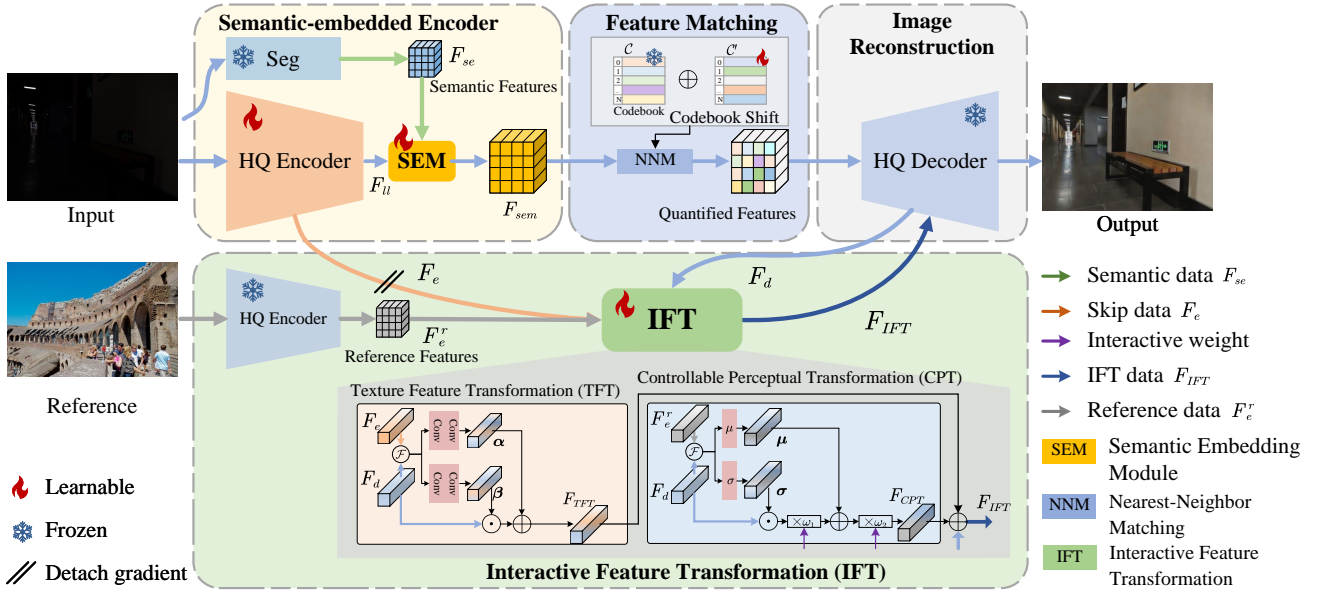


Fig. 2. Overview of the proposed CodeEnhance. We utilize the codebook prior and frozen HQ decoder, both of which are learned in Stage I, as a basis for our design. To improve feature learning, an SEM is introduced to bridge the semantic gap between the output of the HQ encoder and the prior. Meanwhile, a CS mechanism is proposed to overcome the distribution shift among datasets and focus more on valuable priors for LLIE. Additionally, we propose an IFT module performed by a TFT and a CPT to refine texture, color, and illumination.

III. METHODOLOGY

The core idea of our CodeEnhance is to improve the mapping from LL images to HQ images by exploiting a discrete representation space while refining the texture and color information for HQ images. The training process of the CodeEnhance involves two stages. In Stage I, a VQ-GAN [18] is trained to learn a discrete codebook prior and its corresponding decoder. As shown in Fig. 2, an SEM is first designed to ensure effective feature alignment between the learnable HQ encoder and the codebook in the Stage II. Then, a CS mechanism is introduced to fine-tune the codebook based on the Stage II dataset to improve feature matching. Finally, we present an IFT module to improve high-quality details and refine visual perceptual.

A. High-quality Codebook Learning

We first pre-train a VQ-GAN [18] using HQ images to learn a discrete codebook. This codebook serves as prior knowledge for the Stage II. The corresponding HQ decoder of the codebook is used to reconstruct HQ images. Given a HQ image I_h , it is first processed by the HQ encoder of VQ-GAN to obtain a latent feature $\mathbf{Z}_h \in \mathbb{R}^{m \times n \times d}$. Then, by calculating the distance between each ‘pixel’ $z_h^{(i,j)}$ of \mathbf{Z}_h and the c_k in the learnable codebook $\mathbf{C} = \{c_k \in \mathbb{R}^d\}_{k=0}^N$, we replace each $z_h^{(i,j)}$ with the nearest c_k [16]. After that, the quantized features are obtained $\mathbf{Z}_q \in \mathbb{R}^{m \times n \times d}$.

$$z_q^{(i,j)} = \arg \min_{c_k \in \mathbf{C}} \|z_h^{(i,j)} - c_k\|_2, \quad (1)$$

where $N = 1024$ is the codebook size, $d = 512$ denotes the channel number of \mathbf{Z}_h and \mathbf{C} . m and n are the sizes of \mathbf{Z}_h and \mathbf{Z}_q . Finally, the reconstructed image I'_h is produced by the HQ decoder. The VQ-GAN is supervised by \mathcal{L}_{vq} [18], including

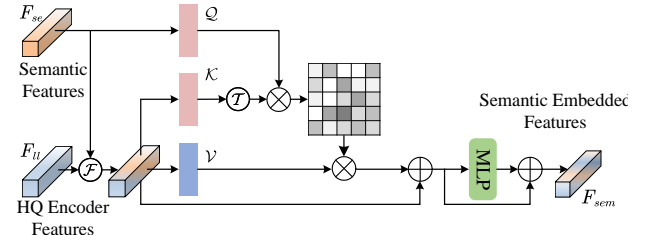


Fig. 3. Overview of our Semantic Embedding Module (SEM).

L1 loss \mathcal{L}_{mae} , codebook matching loss \mathcal{L}_{cma} and adversarial loss \mathcal{L}_{adv} :

$$\begin{aligned} \mathcal{L}_{vq} &= \mathcal{L}_{mae} + \mathcal{L}_{cma} + \mathcal{L}_{adv}, \\ \mathcal{L}_{L1} &= \|I_h - I'_h\|_1, \\ \mathcal{L}_{cma} &= \beta \|\mathbf{Z}_h - \text{sg}(\mathbf{Z}_q)\|_2^2 + \|\text{sg}(\mathbf{Z}_h) - \mathbf{Z}_q\|_2^2, \\ \mathcal{L}_{adv} &= \gamma \log \mathcal{D}(I_h) + \log(1 - \mathcal{D}(I'_h)), \end{aligned} \quad (2)$$

where $\mathcal{D}(\cdot)$ is the discriminator. $\text{sg}(\cdot)$ represents the stop-gradient operator. $\beta = 0.25$ denotes a weight trade-off parameter that governs the update rates of both the encoder and codebook [16]. γ is set to 0.1 [32].

B. Feature Matching via Semantic Embedding and Codebook Shift

This section focuses on optimizing feature matching in the codebook by designing a semantic-embedded encoder SEE(\cdot) comprising an LL encoder and a key component SEM. Additionally, we propose a Codebook Shift (CS) mechanism CS(\cdot) to ensure distribution consistency between the codebook and the current dataset. These techniques improve accuracy

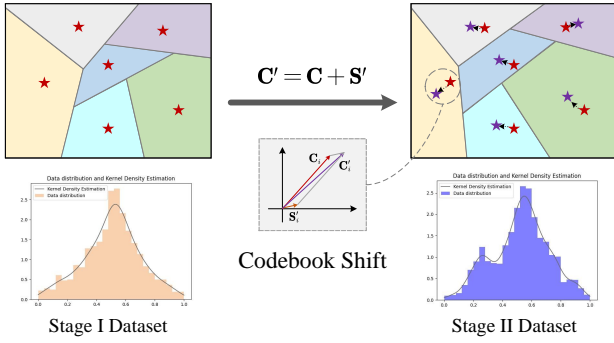


Fig. 4. Overview of the proposed Codebook Shift (CS). The Stage I dataset consists of DIV2K [36] and Flickr2K [37]. The Stage II dataset is LSRW Huawei [38]. The static analysis is based on t-SNE and kernel density estimation.

and robustness in feature matching. The quantized feature $\mathbf{Z}_{ll}^q \in \mathbb{R}^{m \times n \times d}$ of LL image I_{ll} can be obtained by:

$$\hat{z}_q^{(i,j)} = \arg \min_{c_k \in \mathbf{C}} \|\text{SEE}(I_{ll})^{(i,j)} - \text{CS}(\mathbf{C})_k\|_2. \quad (3)$$

Semantic Embedding Module. Affected by noise and illumination, features in LL images are distorted, resulting in difficult generalization of the original HQ encoder and a semantic gap between the HQ encoder output and the priors. To tackle these challenges, we integrate semantic information and the output of the HQ encoder through a novel SEM. This module compensates for semantic information and enhances the overall learning quality.

As illustrated in Figs. 2 and 3, we use a pre-trained semantic segmentation network (e.g., DeepLab v3 [35]) to extract the semantic feature \mathbf{F}_{se} from the input image. Moreover, we use the learnable HQ encoder to obtain \mathbf{F}_{ll} . Subsequently, the \mathbf{F}_{ll} and \mathbf{F}_{se} are sent to the SEM. Within SEM, \mathbf{F}_{se} and \mathbf{F}_{ll} are fused at first, followed by using fused features and \mathbf{F}_{se} to compute an attention-weight map. This map is then applied to the fused features to suppress noise information and obtain semantically embedded features. Lastly, the features are processed by a Multi-Layer Perceptron (MLP) [29]. The SEM can be represented as:

$$\begin{aligned} \mathbf{M} &= \mathcal{Q}(\mathbf{F}_{se})\mathcal{K}([\mathbf{F}_{se}, \mathbf{F}_{ll}]^T), \\ \mathbf{F}' &= \mathcal{V}([\mathbf{F}_{se}, \mathbf{F}_{ll}])\mathbf{M} + [\mathbf{F}_{se}, \mathbf{F}_{ll}], \\ \mathbf{F}_{sem} &= \text{MLP}(\mathbf{F}') + \mathbf{F}', \end{aligned} \quad (4)$$

where $\mathcal{Q}(\cdot)$, $\mathcal{K}(\cdot)$, and $\mathcal{V}(\cdot)$ denote the computing of query, key, and value for obtaining attention-weight map \mathbf{M} . $(\cdot)^T$ is transpose operation, and $[\cdot, \cdot]$ represents feature concatenation in channel dimension.

Codebook Shift. The codebook priors, which consist of HQ image features, act as representative class centers for the Stage I dataset [18], [30]. However, as depicted in Fig. 4, there may be a distribution shift between the Stage I and Stage II datasets, presenting a challenge for feature matching. Furthermore, different priors have various contributions to feature matching. But most existing methods use the priors without distinction [16], [32], which leads to performance degradation in feature matching. As shown in Fig. 4, to tackle these challenges, we introduce a Codebook Shift (CS) mechanism, which aims to ensure distribution consistency between the codebook and the

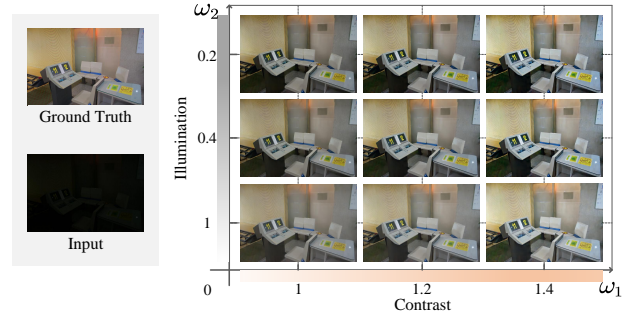


Fig. 5. Results under various adjustment degrees. Our IFT allows users to adjust the enhancement in terms of color and illumination by adjusting the ω_1 and ω_2 .

dataset in Stage II and focus more on valuable priors for LLIE. The CS can be formulated as follows:

$$\mathbf{C}' = \mathbf{C} + \mathbf{S}', \quad (5)$$

where $\mathbf{C}' \in \mathbb{R}^{N \times d}$ denotes the new codebook. $\mathbf{S}' \in \mathbb{R}^{N \times d}$ is the learnable shift.

Controllable Perceptual Transformation. To enhance the contrast and brightness of the enhanced image, we utilize a high-quality image with proper colors and illumination intensities as a reference for guidance. This reference image serves as valuable information for the model to learn perceptual details. In this way, we introduce a CPT that extracts contrast and brightness information from the reference images and integrates it into the restoration process. As depicted in Fig. 2, the reference image is sent to the pre-trained frozen HQ encoder to obtain reference features \mathbf{F}_e^r . The CPT can be formulated as follows:

$$\mathbf{F}_{CPT} = \omega_1(\sigma \mathbf{F}_d) + \omega_2 \boldsymbol{\mu}, \quad (6)$$

where as shown in Fig. 5, ω_1 and ω_2 are used to control the impact of the CPT in contrast and brightness, respectively. Given a feature $\mathbf{F}' = [\mathbf{F}_d, \mathbf{F}_e^r]$, $\mathbf{F}' \in \mathbb{R}^{B \times C \times H \times W}$. The $\sigma = [\sigma_{bc}]_{B \times C}$ and $\boldsymbol{\mu} = [\mu_{bc}]_{B \times C}$ are computed across spatial locations [39], which can be formulated as follows:

$$\begin{aligned} \mu_{bc} &= \frac{1}{HW} \sum_{h=1}^H \sum_{w=1}^W \mathbf{F}'_{bchw}, \\ \sigma_{bc} &= \sqrt{\frac{1}{HW} \sum_{h=1}^H \sum_{w=1}^W (\mathbf{F}'_{bchw} - \mu_{bc})^2}. \end{aligned} \quad (7)$$

where Intuitively, a channel feature is regarded as a perceptron that represents a specific style of information [39]. Images with this style will exhibit higher activation rates on the corresponding channel. By extracting the mean and variance of the channel, the CPT module captures contrast and brightness information associated with the channel. This enables CPT to obtain more nuanced perceptual information while preserving the original content of the image. In essence, CPT controls the transmission of perceptual information in the feature space by utilizing feature statistics (e.g., variance and mean).

TABLE I

QUANTITATIVE COMPARISONS ON LSRW [38] (NIKON AND HUAWEI), FIVEK [41], LOL [1], AND SYNLL [24]. ↑ INDICATES THE HIGHER THE BETTER, ↓ INDICATES THE LOWER THE BETTER.

Methods	Metrics	LIME [42]	JED [43]	RetinexNet [1]	KinD [44]	Zero [45]	EnGAN [12]	SNR [2]	MIRNetv2 [4]	PairLIE [46]	SMG [3]	Ours
Nikon	PSNR↑	14.44	14.79	13.49	15.36	15.04	14.63	16.63	17.10	15.52	17.26	17.31
	SSIM↑	0.3554	0.4600	0.2934	0.4271	0.4198	0.3984	0.5052	0.5125	0.4346	0.4927	0.5061
	LPIPS↓	0.3303	0.3510	0.4041	0.3444	0.3763	0.3248	0.5025	0.4516	0.3225	0.3343	0.2610
	MAE↓	0.1442	0.1572	0.1758	0.1430	0.1506	0.1518	0.1247	0.1233	0.1360	0.1134	0.1086
Huawei	PSNR↑	18.46	15.11	16.82	17.19	16.40	17.46	20.40	20.12	18.99	20.77	21.14
	SSIM↑	0.4450	0.5379	0.3951	0.4625	0.4761	0.4982	0.6167	0.6317	0.5632	0.4880	0.6076
	LPIPS↓	0.3923	0.4327	0.4566	0.4318	0.3212	0.3780	0.4879	0.4307	0.3711	0.4193	0.2840
	MAE↓	0.0950	0.1524	0.1186	0.1155	0.1342	0.1121	0.0784	0.0816	0.0920	0.0726	0.0733
FiveK	PSNR↑	11.51	14.44	12.30	13.75	13.50	9.33	23.85	24.11	10.55	24.08	24.69
	SSIM↑	0.6869	0.7184	0.6874	0.7283	0.7022	0.6459	0.8858	0.9007	0.6371	0.8756	0.9023
	LPIPS↓	0.1802	0.1947	0.2249	0.1715	0.2084	0.2507	0.1340	0.0843	0.2695	0.1415	0.0750
	MAE↓	0.2491	0.1715	0.2026	0.1776	0.1845	0.3254	0.0623	0.0591	0.2710	0.0581	0.0536
LOL	PSNR↑	17.18	13.69	16.77	14.78	14.86	18.68	24.61	24.74	18.47	24.30	22.90
	SSIM↑	0.4747	0.6577	0.4191	0.5520	0.5588	0.6531	0.8419	0.8480	0.7473	0.8093	0.8424
	LPIPS↓	0.3419	0.2933	0.4047	0.4506	0.3218	0.3224	0.2064	0.1725	0.2899	0.2352	0.1268
	MAE↓	0.1242	0.2108	0.1256	0.1750	0.1846	0.1161	0.0552	0.0575	0.1153	0.0557	0.0783
SynLL	PSNR↑	13.84	13.07	12.99	16.41	13.79	16.66	22.54	22.55	16.59	22.94	23.32
	SSIM↑	0.3746	0.4017	0.3855	0.4923	0.4217	0.5316	0.7391	0.7577	0.5706	0.7124	0.7793
	LPIPS↓	0.4240	0.4240	0.4568	0.4134	0.3871	0.3979	0.3292	0.2424	0.4019	0.2827	0.1904
	MAE↓	0.1699	0.1963	0.1889	0.1274	0.1881	0.1211	0.0783	0.0627	0.1241	0.0603	0.0559

C. Training Objectives

The training objective consists of three loss functions: Feature Matching Loss, Reconstruction Loss, and Adversarial Loss, which can be formulated as follows:

$$\mathcal{L}_{total} = \mathcal{L}_{fema} + \mathcal{L}_{rec} + \mathcal{L}_{adv} + \lambda_1 \mathcal{L}_{reg}, \quad (8)$$

where \mathcal{L}_{adv} has been defined in Eq. 2 and $\mathcal{L}_{reg} = \|S'\|_2$ denotes L2 regularization term that controls the influence of S' . $\lambda_1 = 10^{-4}$ is a hypeparameter. The other two losses are defined as follows.

Feature Matching Loss. This loss is used to optimize the encoder to learn the mapping between LL images and HQ priors, which can be formulated as follows:

$$\begin{aligned} \mathcal{L}_{fema} = & \beta \| \hat{\mathbf{Z}}_l - \text{sg}(\mathbf{Z}_{gt}) \|_2^2 + \| \phi(\hat{\mathbf{Z}}_l) - \phi(\text{sg}(\mathbf{Z}_{gt})) \|_2^2 \\ & + \| \mathbf{Z}_{ll}^q - \text{sg}(\mathbf{Z}_{gt}^q) \|_2^2, \end{aligned} \quad (9)$$

where $\phi(\cdot)$ is used to calculate the gram matrix of features. $\hat{\mathbf{Z}}_l$ and \mathbf{Z}_{gt} represent the latent features of LL images and ground truth, respectively. \mathbf{Z}_{ll}^q and \mathbf{Z}_{gt}^q denote the quantized features of LL images and ground truth, respectively.

Reconstruction Loss. This loss focuses on ensuring the enhanced images with a completed structure and impressing visual pleasure, which is performed by L1 loss and perceptual loss:

$$\mathcal{L}_{rec} = \|I_{gt} - I_{rec}\|_1 + \|\psi(I_{gt}) - \psi(I_{rec})\|_2^2, \quad (10)$$

where $\psi(\cdot)$ indicates the LPIPS function [40].

IV. EXPERIMENTS

A. Implementation Details

For both the training of VQ-GAN and the proposed method, input image pairs are randomly cropped to obtain the input patches with the size of 256×256 . We use ADAM optimizer [47] with $\beta_1 = 0.9$, $\beta_2 = 0.999$ and $\varepsilon = 10^{-8}$. The learning rate is set to 10^{-4} . The VQ-GAN is pre-trained on the DIV2K [36] and Flickr2K [37] with 350K iterations. Our CodeEnhance is trained on the low-light datasets with 5K

iterations. All experiments are implemented by the PyTorch framework on an NVIDIA A100 GPU.

B. Datasets and Evaluation Metrics

Low-light Datasets. We use LSRW [38], FiveK [41], LOL [1], and SynLL [24] datasets to evaluate the proposed method. The LSRW contains Huawei and Nikon datasets. The Huawei consists of training and testing sets with 2450 and 30, respectively. The Nikon includes 3,150 and 20 image pairs for training and testing, respectively. FiveK [41] dataset consists of 4500 image pairs for training and 500 image pairs for testing. The LOL dataset includes 485 and 15 image pairs for training and testing, respectively. The SynLL [24] benchmark synthesizes 23,431 short/long exposure image pairs by imposing the degradation of illumination, color, and noise. 22,472 and 959 image pairs are used for training and testing.

Object Detection Dataset. ExDark [5] is an LL image dataset for object detection. It contains 7,363 images from multi-level illumination and 12 object classes. We partitioned the dataset according to the strategy outlined in [5], with 3,000 images for training, 1,800 images for validation, and 2563 images for testing.

Evaluation Metrics. We use the most common peak signal-to-noise ratio (PSNR), structural similarity [48] (SSIM), mean abstract error (MAE), and learned perceptual image patch similarity (LPIPS) [40] to measure the quality of the enhanced image. Unlike PSNR and MAE, LPIPS takes into account the human visual system’s perception of similarity, which provides a more accurate assessment of the perceived similarity between images.

C. Comparison with State-of-the-Art Methods

To evaluate the effectiveness of our CodeEnhance, we compare it with several state-of-the-art (SOTA) LLIE methods, including LIME [42], JED [43], RetinexNet [1], KinD [44], EnGAN [12], Zero [45], SNR [2], MIRNet v2 [4], PairLIE [46], SMG [3], from both quantitative and qualitative perspectives.

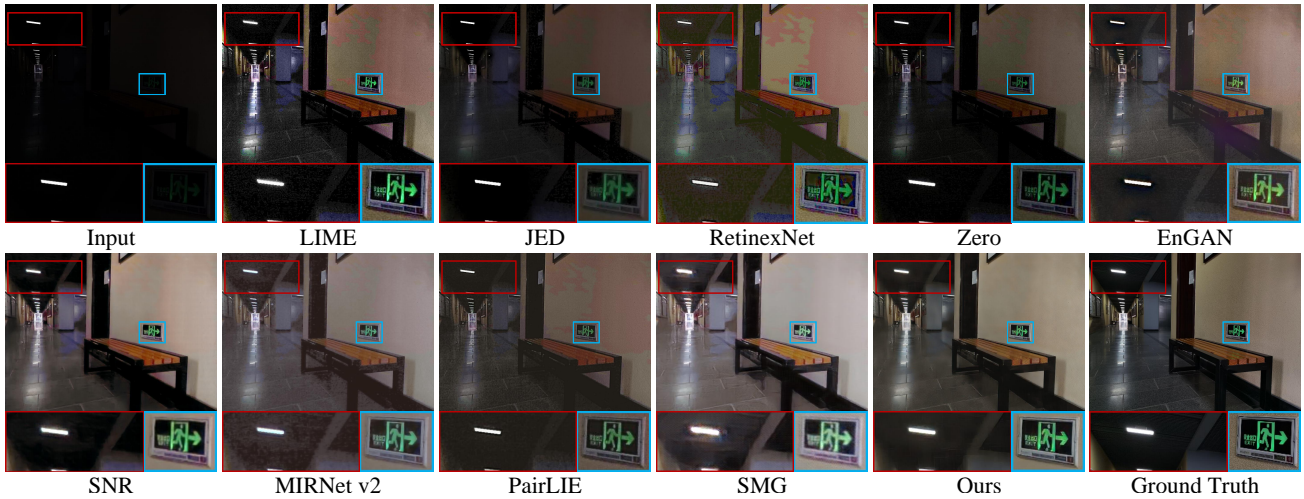


Fig. 6. Visual comparisons on the LSRW Huawei [38] dataset. Our results exhibit minimal artifacts and the most accurate color restoration.

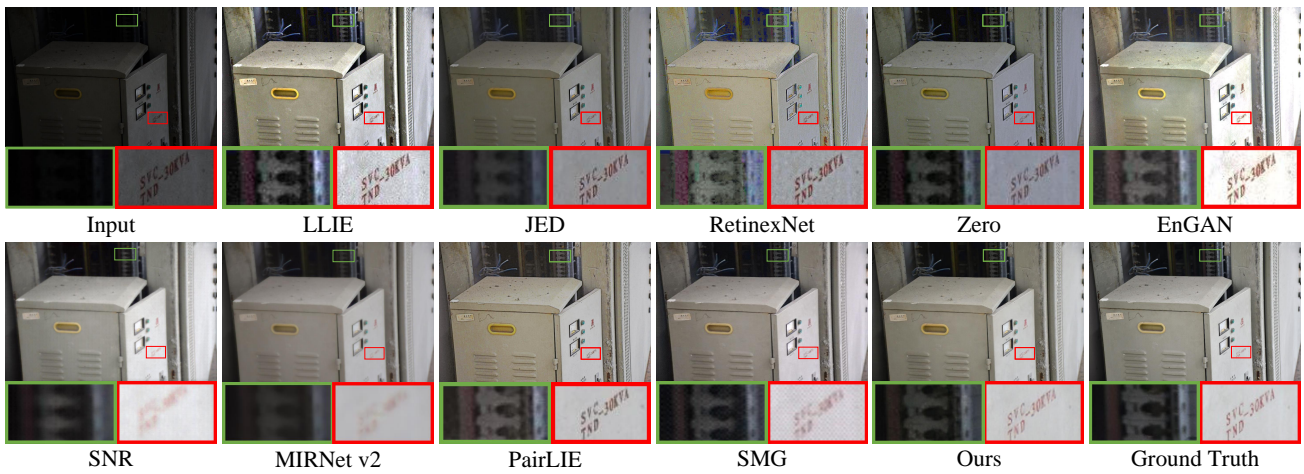


Fig. 7. Visual comparisons on the LSRW Nikon [38] dataset. Our results strike a trade-off between noise suppression and texture preservation while maintaining color authenticity.



Fig. 8. Visual comparisons on the FiveK [41] dataset. Our results are the closest to the ground truth regarding illumination, color, and texture.

As shown in Tabel. I, we compare the proposed CodeEnhance against SOTA LLIE methods regarding PSNR, SSIM, MAE, and LPIPS on the LOL, LSRW (Huawei and Nikon), FiveK, and SynLL datasets. In the case where the LL images contain much noise [1] [24], some methods typically over-smooth the noise, leading to higher PSNR [2] [4] [3]. However,

as shown in Figs. 6-9, they often lack high-frequency detail information and have poor perceptual quality, while the proposed CodeEnhance can obtain perceptually more convincing results, as indicated by the lowest LPIPS score. Figs. 6-9 show visual results comparisons. In a fully dark scene (Fig. 6 and Fig. 9), SNR and SMG improve overall brightness but introduce noise

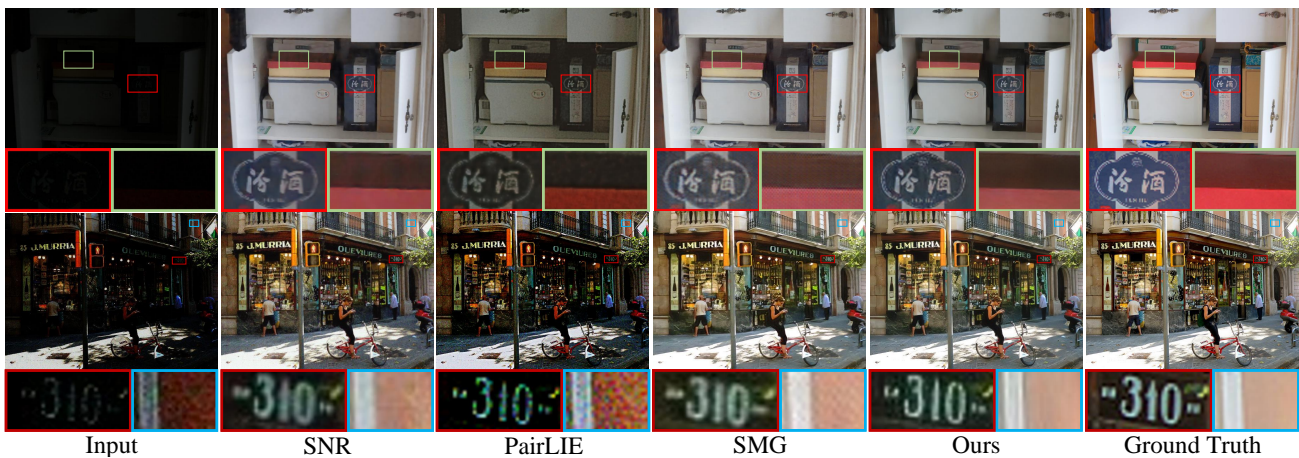


Fig. 9. Visual comparisons on the LOL [1] and SynLL [24]. Our CodeEnhance has less noise and more texture.

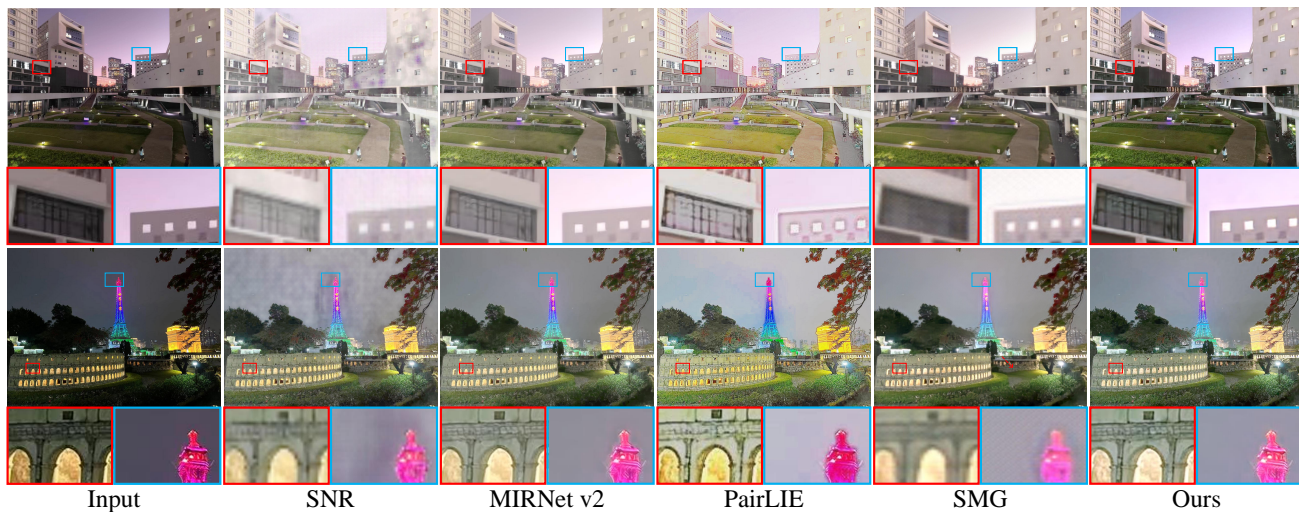


Fig. 10. Visual results on the real scene. The results demonstrate the superior performance of our proposed CodeEnhance method. Particularly, it excels in preserving texture details and effectively handling gradient change regions.

and artifacts, which damage the image quality. In scenes with uneven illumination (Fig. 7 and Fig. 8), methods like JED, KinD, and PairLIE enhance brightness better but suffer from color distortion and lack of details. SNR and SMG are susceptible to issues such as local color deviation and loss of texture. In contrast, our method enhances image illumination, not only suppressing noise and artifacts, but also accurately restoring color and texture information. Intuitively, the text in the figures appears significantly clearer, significantly improving the visual perception. This is accomplished by utilizing HQ image priors and incorporating advanced components such as SEM, CS, and IFT in our design.

Additionally, our method also has a superior performance in real scenes. Fig. 10 illustrates that our method achieves smooth processing in areas with a wide dynamic range of illumination changes (e.g., gradient sky colors and the transition between buildings and the sky, as depicted in Fig. 10). It effectively avoids artifacts and color deviation, resulting in visually pleasing and artifact-free enhancements. This demonstrates the robustness and effectiveness of our method in handling challenging scenarios with varying illumination conditions. Meanwhile, our method can adaptively enhance

TABLE II
RUNTIME ON LSRW NIKON DATASET [38].

Methods	JED [43]	RetinexNet [1]	KinD [44]	Zero [45]	EnGAN [12]
Runtime (s)	6.8399	0.8435	1.4771	0.0018	0.2151
Methods	SNR [2]	MIRNet v2 [4]	PairLIE [46]	SMG [3]	Ours
Runtime (s)	0.3092	0.2349	0.0525	0.5897	0.0330

low-illumination areas instead of uniformly enhancing all dark areas. This adaptive approach helps to avoid amplifying noise and enables us to achieve excellent contrast while enhancing brightness. In addition, Table II demonstrates that our approach well trade-offs efficiency and image enhancement quality.

D. Low-light Object Detection

Although LLIE preprocessing improves the overall illumination and visual perception of low-light images, it may also potentially degrade image features. Specifically, when the features of enhanced images are not effectively preserved or enhanced, the LLIE methods negatively impact the performance of high-level tasks. To mitigate this impact, it is important to consider enhancing edges, textures, and object details [49].



Fig. 11. Comparisons of the improvement on object detection tasks [5]. Our method not only enhances the image quality but also improves the performance of object detection algorithms.

TABLE III
THE MEAN AVERAGE PRECISION (MAP) COMPARISONS OF LOW-LIGHT OBJECT DETECTION ON ExDARK [5].

Methods	Bicycle	Boat	Bottle	Bus	Car	Cat	Chair	Cup	Dog	Motor	People	Table	mAP
LIME [42] ²⁰¹⁶	82.75	77.59	73.92	90.12	83.6	67.22	69.51	74.01	78.29	64.05	80.95	54.24	74.68
JED [43] ²⁰¹⁸	82.74	76.74	74.32	85.57	81.07	67.89	68.56	73.64	79.79	65.84	80.4	54.21	74.23
RetinexNet [1] ²⁰¹⁸	81.97	77.59	74.08	85.68	79.61	54.92	63.32	71.28	66.39	59.08	77.59	51.17	70.22
KinD [44] ²⁰¹⁹	81.13	78.04	74.97	87.96	82.69	59.95	66.62	72.4	72.25	63.69	80.28	50.44	72.54
Zero [45] ²⁰²⁰	83.44	77.22	75.17	89.7	82.4	62.67	66.8	73.17	75.68	64.16	80.68	50.22	73.44
EnGAN [12] ²⁰²¹	81.68	76.39	74.83	89.44	80.16	63.81	65.57	72.53	77.18	64.24	80.55	51.51	73.16
SNR [2] ²⁰²²	83.65	77.44	72.97	89.01	82.7	62.64	66.51	71.02	74.91	64.74	80.19	50.55	73.03
MIRNet v2 [4] ²⁰²³	85.02	79.35	74.27	90.68	82.91	66.36	67.87	70.14	79	64.76	80.67	55.6	74.72
PairLIE [46] ²⁰²³	82.87	77.38	72	88.11	82.38	62.03	70.23	70.44	76.31	64.1	80.11	54.95	73.41
SMG [3] ²⁰²³	82.05	76.51	71.71	88.07	79.11	64.97	66.84	68.32	77.69	63.16	77.88	53.78	72.51
Ours	84.08	78.58	75.08	88.95	82.33	67.12	68.62	74.19	78.85	63.63	81.71	53.83	74.75

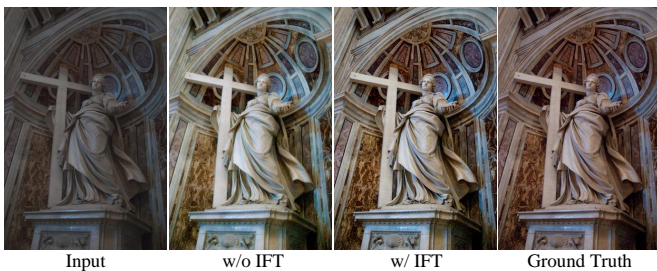


Fig. 12. Visualized ablation of IFT on FiveK.

To assess the impact of our method in enhancing the performance of high-level tasks under low-light conditions, we utilize YOLOv7 [50] as the object detector and train it on the ExDark dataset, which was preprocessed using the LLIE methods. The comparison of Average Precision (AP) is presented in Table III, revealing that our method yields images that better facilitate the learning of the target detection algorithm. Furthermore, Fig. 11 demonstrates the effectiveness of our method in suppressing noise while increasing overall brightness in images with complex scenes. As a result, high-quality enhanced images obtained by the proposed CodeEnhance enable YOLOv7 to extract more valuable information and achieve better detection performance.

E. Ablation Study

To verify the effectiveness of the core modules of our CodeEnhance, we conduct a series of ablation studies. The Baseline model is constructed by a VQ-GAN [18].

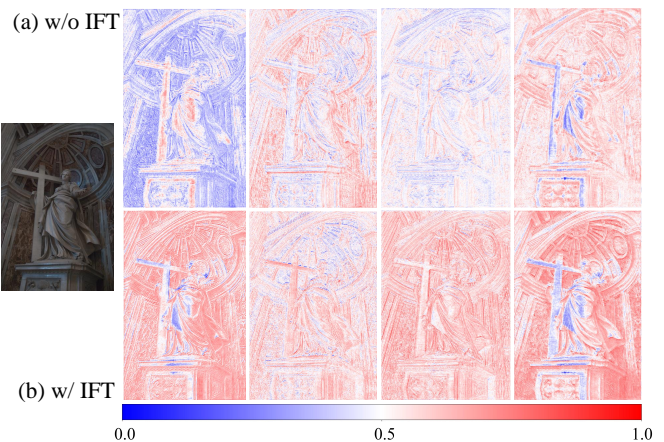


Fig. 13. Visual of feature maps. The higher the feature activation, the greater the feature score. It is evident that our IFT (bottom) enhances CodeEnhance’s ability to capture more texture information.

Study of SEM. According to the Table IV, we first assess the proposed SEM. The results show that SEM effectively enhances the model’s performance. For example, when compared to Exp. (a) using the baseline model, PSNR and SSIM increased by 0.33 and 0.0152, respectively. These results indicate that SEM can acquire high-quality image features, thereby enhancing the accuracy of feature matching so as to improve overall model performance.

Study of IFT. IFT consists of a TFT and a CPT, and we will evaluate their effectiveness individually. Figs. 5, 12, and 13, and Table IV demonstrate that the proposed IFT and CPT can

TABLE IV
ABLATION STUDIES OF THE CODEENHANCE ON FIVEK [41] DATASET.
THE BASELINE MODEL IS BUILT BY A VQ-GAN [18]

Exp.	Baseline	SEM	IFT		CS	PSNR	SSIM
			TFT	CPT			
(a)	✓					22.84	0.8693
(b)	✓	✓				23.17	0.8845
(c)	✓	✓	✓			24.16	0.8955
(d)	✓	✓	✓	✓		24.53	0.9012
(e)	✓	✓	✓	✓	✓	24.69	0.9023

TABLE V
ABLATION STUDIES OF IFT, REFERENCE IMAGE, AND CODEBOOK.

Model	Baseline	Baseline + IFT	w/o Refer Img	w/o codebook	Ours
PSNR	22.84	24.01	24.23	21.46	24.69
SSIM	0.8693	0.8893	0.8960	0.8227	0.9023

TABLE VI
ABLATION STUDIES OF THE λ_1 FOR \mathcal{L}_{reg} .

λ_1	0	0.01	0.001	0.0001
PSNR	24.46	24.65	24.48	24.69
SSIM	0.9008	0.9006	0.9014	0.9023

improve the performance of our CodeEnhance significantly. For instance, when compared to Exp. (b) in Table IV, there is a PSNR increase of 1.36 and an SSIM increase of 0.0167. These findings validate the effectiveness of our IFT in effectively controlling texture, color, and illumination information, thereby enhancing the overall model performance.

Study of CS. CS is designed to rectify distribution discrepancies among various datasets. As demonstrated in Table IV (Exp. (d) and (e)) and Table VI, CS has a beneficial impact on the model, resulting in an improvement of 0.16 in PSNR. This indicates that CS can effectively fine-tune the Codebook, adapting it to the current dataset and enhancing the model’s performance.

V. CONCLUSION

In conclusion, we present a novel LLIE method, CodeEnhance, to obtain HQ images from LL images. We redefine LLIE as learning an image-to-code mapping between LL images and discrete codebook priors. Our method includes the Semantic Embedding Module (SEM) and Codebook Shift (CS) mechanism to enhance mapping learning by integrating semantic information and ensuring distribution consistency in feature matching. Additionally, the Interactive Feature Transformation (IFT) module improves texture and color information in image reconstruction, allowing interactive adjustment based on user preferences. Experimental results on real-world and synthetic benchmarks demonstrate that our approach improves LLIE performance in terms of quality, fidelity, and robustness to various degradations.

REFERENCES

- [1] C. Wei, W. Wang, W. Yang, and J. Liu, “Deep retinex decomposition for low-light enhancement,” in *British Machine Vision Conference*, 2018.
- [2] X. Xu, R. Wang, C.-W. Fu, and J. Jia, “Snr-aware low-light image enhancement,” in *2022 IEEE/CVF Conference on Computer Vision and Pattern Recognition*, 2022, pp. 17 693–17 703.
- [3] X. Xu, R. Wang, and J. Lu, “Low-light image enhancement via structure modeling and guidance,” in *2023 IEEE/CVF Conference on Computer Vision and Pattern Recognition*, 2023, pp. 9893–9903.
- [4] S. W. Zamir, A. Arora, S. Khan, M. Hayat, F. S. Khan, M.-H. Yang, and L. Shao, “Learning enriched features for fast image restoration and enhancement,” *IEEE Transactions on Pattern Analysis and Machine Intelligence*, vol. 45, no. 2, pp. 1934–1948, 2023.
- [5] Y. P. Loh and C. S. Chan, “Getting to know low-light images with the exclusively dark dataset,” *Computer Vision and Image Understanding*, vol. 178, pp. 30–42, 2019.
- [6] K. G. Lore, A. Akintayo, and S. Sarkar, “Llnet: A deep autoencoder approach to natural low-light image enhancement,” *Pattern Recognition*, vol. 61, pp. 650–662, 2017.
- [7] S. M. Pizer, E. P. Amburn, J. D. Austin, R. Cromartie, A. Geselowitz, T. Greer, B. ter Haar Romeny, J. B. Zimmerman, and K. Zuiderveld, “Adaptive histogram equalization and its variations,” *Computer vision, graphics, and image processing*, vol. 39, no. 3, pp. 355–368, 1987.
- [8] D. Jobson, Z. Rahman, and G. Woodell, “Properties and performance of a center/surround retinex,” *IEEE Transactions on Image Processing*, vol. 6, no. 3, pp. 451–462, 1997.
- [9] E. H. Land and J. J. McCann, “Lightness and retinex theory,” *Journal of the Optical Society of America*, vol. 61 1, pp. 1–11, 1971.
- [10] R. Wan, B. Shi, W. Yang, B. Wen, L.-Y. Duan, and A. C. Kot, “Purifying low-light images via near-infrared enlightened image,” *IEEE Transactions on Multimedia*, vol. 25, pp. 8006–8019, 2023.
- [11] J. Xu, M. Yuan, D.-M. Yan, and T. Wu, “Illumination guided attentive wavelet network for low-light image enhancement,” *IEEE Transactions on Multimedia*, vol. 25, pp. 6258–6271, 2023.
- [12] Y. Jiang, X. Gong, D. Liu, Y. Cheng, C. Fang, X. Shen, J. Yang, P. Zhou, and Z. Wang, “Enlightengan: Deep light enhancement without paired supervision,” *IEEE Transactions on Image Processing*, vol. 30, pp. 2340–2349, 2021.
- [13] K. Wu, J. Huang, Y. Ma, F. Fan, and J. Ma, “Cycle-retinex: Unpaired low-light image enhancement via retinex-inline cyclegan,” *IEEE Transactions on Multimedia*, vol. 26, pp. 1213–1228, 2024.
- [14] L. Ma, R. Liu, J. Zhang, X. Fan, and Z. Luo, “Learning deep context-sensitive decomposition for low-light image enhancement,” *IEEE Transactions on Neural Networks and Learning Systems*, vol. 33, no. 10, pp. 5666–5680, 2022.
- [15] S. Lin, F. Tang, W. Dong, X. Pan, and C. Xu, “Smnet: Synchronous multi-scale low light enhancement network with local and global concern,” *IEEE Transactions on Multimedia*, vol. 25, pp. 9506–9517, 2023.
- [16] S. Zhou, K. Chan, C. Li, and C. C. Loy, “Towards robust blind face restoration with codebook lookup transformer,” in *Advances in Neural Information Processing Systems*, vol. 35, 2022, pp. 30 599–30 611.
- [17] T. Zhao and X. Wu, “Pyramid feature attention network for saliency detection,” in *2019 IEEE/CVF Conference on Computer Vision and Pattern Recognition*, 2019, pp. 3080–3089.
- [18] P. Esser, R. Rombach, and B. Ommer, “Taming transformers for high-resolution image synthesis,” in *2021 IEEE/CVF Conference on Computer Vision and Pattern Recognition*, 2021, pp. 12 868–12 878.
- [19] S. Hao, X. Han, Y. Guo, X. Xu, and M. Wang, “Low-light image enhancement with semi-decoupled decomposition,” *IEEE Transactions on Multimedia*, vol. 22, no. 12, pp. 3025–3038, 2020.
- [20] T. Celik and T. Tjahjadi, “Contextual and variational contrast enhancement,” *IEEE Transactions on Image Processing*, vol. 20, no. 12, pp. 3431–3441, 2011.
- [21] J. Stark, “Adaptive image contrast enhancement using generalizations of histogram equalization,” *IEEE Transactions on Image Processing*, vol. 9, no. 5, pp. 889–896, 2000.
- [22] T. Arici, S. Dikbas, and Y. Altunbasak, “A histogram modification framework and its application for image contrast enhancement,” *IEEE Transactions on Image Processing*, vol. 18, no. 9, pp. 1921–1935, 2009.
- [23] L. Ma, R. Liu, Y. Wang, X. Fan, and Z. Luo, “Low-light image enhancement via self-reinforced retinex projection model,” *IEEE Transactions on Multimedia*, vol. 25, pp. 3573–3586, 2023.
- [24] F. Lv, Y. Li, and F. Lu, “Attention guided low-light image enhancement with a large scale low-light simulation dataset,” *International Journal of Computer Vision*, vol. 129, no. 7, pp. 2175–2193, 2021.
- [25] X. Wu, Z. Lai, S. Yu, J. Zhou, Z. Liang, and L. Shen, “Coarse-to-fine low-light image enhancement with light restoration and color refinement,” *IEEE Transactions on Emerging Topics in Computational Intelligence*, pp. 1–13, 2023.
- [26] L. Ma, T. Ma, R. Liu, X. Fan, and Z. Luo, “Toward fast, flexible, and robust low-light image enhancement,” in *2022 IEEE/CVF Conference on Computer Vision and Pattern Recognition*, 2022, pp. 5627–5636.

- [27] W. Wu, J. Weng, P. Zhang, X. Wang, W. Yang, and J. Jiang, "Uretinex-net: Retinex-based deep unfolding network for low-light image enhancement," in *2022 IEEE/CVF Conference on Computer Vision and Pattern Recognition*, 2022, pp. 5891–5900.
- [28] Y. Cai, H. Bian, J. Lin, H. Wang, R. Timofte, and Y. Zhang, "Retinex-former: One-stage retinex-based transformer for low-light image enhancement," in *2023 Proceedings of the IEEE/CVF International Conference on Computer Vision*, October 2023, pp. 12 504–12 513.
- [29] A. Vaswani, N. Shazeer, N. Parmar, J. Uszkoreit, L. Jones, A. N. Gomez, Ł. Kaiser, and I. Polosukhin, "Attention is all you need," in *2017 Conference on Neural Information Processing Systems*, 2017, pp. 5998–6008.
- [30] A. van den Oord, O. Vinyals, and k. kavukcuoglu, "Neural discrete representation learning," in *Advances in Neural Information Processing Systems*, vol. 30, 2017.
- [31] C. Chen, X. Shi, Y. Qin, X. Li, X. Han, T. Yang, and S. Guo, "Real-world blind super-resolution via feature matching with implicit high-resolution priors," in *2022 ACM International Conference on Multimedia*, 2022.
- [32] R.-Q. Wu, Z.-P. Duan, C.-L. Guo, Z. Chai, and C. Li, "Ridcp: Revitalizing real image dehazing via high-quality codebook priors," in *2023 IEEE/CVF Conference on Computer Vision and Pattern Recognition*, 2023, pp. 22 282–22 291.
- [33] B. Guo, X. Zhang, H. Wu, Y. Wang, Y. Zhang, and Y.-F. Wang, "Larsr: A local autoregressive model for image super-resolution," in *2022 IEEE/CVF Conference on Computer Vision and Pattern Recognition*, 2022, pp. 1899–1908.
- [34] Y. Gu, X. Wang, L. Xie, C. Dong, G. Li, Y. Shan, and M.-M. Cheng, "Vqfr: Blind face restoration with vector-quantized dictionary and parallel decoder," in *2022 European Conference on Computer Vision*. Springer, 2022, pp. 126–143.
- [35] L.-C. Chen, G. Papandreou, F. Schroff, and H. Adam, "Rethinking atrous convolution for semantic image segmentation," *arXiv preprint arXiv:1706.05587*, 2017.
- [36] E. Agustsson and R. Timofte, "Ntire 2017 challenge on single image super-resolution: Dataset and study," in *2017 IEEE Conference on Computer Vision and Pattern Recognition Workshops*, 2017, pp. 1122–1131.
- [37] B. Lim, S. Son, H. Kim, S. Nah, and K. M. Lee, "Enhanced deep residual networks for single image super-resolution," in *2017 IEEE Conference on Computer Vision and Pattern Recognition Workshops*, 2017, pp. 1132–1140.
- [38] J. Hai, Z. Xuan, R. Yang, Y. Hao, F. Zou, F. Lin, and S. Han, "R2rnet: Low-light image enhancement via real-low to real-normal network," *Journal of Visual Communication and Image Representation*, vol. 90, p. 103712, 2023.
- [39] X. Huang and S. Belongie, "Arbitrary style transfer in real-time with adaptive instance normalization," in *2017 IEEE International Conference on Computer Vision*, 2017, pp. 1510–1519.
- [40] R. Zhang, P. Isola, A. A. Efros, E. Shechtman, and O. Wang, "The unreasonable effectiveness of deep features as a perceptual metric," in *2018 IEEE/CVF Conference on Computer Vision and Pattern Recognition*, 2018, pp. 586–595.
- [41] V. Bychkovsky, S. Paris, E. Chan, and F. Durand, "Learning photographic global tonal adjustment with a database of input / output image pairs," in *2011 IEEE/CVF Conference on Computer Vision and Pattern Recognition*, 2011, pp. 97–104.
- [42] X. Guo, Y. Li, and H. Ling, "Lime: Low-light image enhancement via illumination map estimation," *IEEE Transactions on Image Processing*, vol. 26, no. 2, pp. 982–993, 2016.
- [43] X. Ren, M. Li, W.-H. Cheng, and J. Liu, "Joint enhancement and denoising method via sequential decomposition," in *the IEEE International Symposium on Circuits and Systems*, 2018, pp. 1–5.
- [44] Y. Zhang, J. Zhang, and X. Guo, "Kindling the darkness: A practical low-light image enhancer," in *2019 Proceedings of the ACM international conference on multimedia*, 2019, pp. 1632–1640.
- [45] C. Guo, C. Li, J. Guo, C. C. Loy, J. Hou, S. Kwong, and R. Cong, "Zero-reference deep curve estimation for low-light image enhancement," in *the IEEE/CVF Conference on Computer Vision and Pattern Recognition*, 2020, pp. 1780–1789.
- [46] Z. Fu, Y. Yang, X. Tu, Y. Huang, X. Ding, and K.-K. Ma, "Learning a simple low-light image enhancer from paired low-light instances," in *2023 IEEE/CVF Conference on Computer Vision and Pattern Recognition*, 2023, pp. 22 252–22 261.
- [47] D. P. Kingma and J. Ba, "Adam: A method for stochastic optimization," in *2015 International Conference on Learning Representations*, Y. Bengio and Y. LeCun, Eds., 2015.
- [48] Z. Wang, A. Bovik, H. Sheikh, and E. Simoncelli, "Image quality assessment: from error visibility to structural similarity," *IEEE Transactions on Image Processing*, vol. 13, no. 4, pp. 600–612, 2004.
- [49] W. Liu, G. Ren, R. Yu, S. Guo, J. Zhu, and L. Zhang, "Image-adaptive yolo for object detection in adverse weather conditions," in *2022 Proceedings of the AAAI Conference on Artificial Intelligence*, vol. 36, no. 2, 2022, pp. 1792–1800.
- [50] C.-Y. Wang, A. Bochkovskiy, and H.-Y. M. Liao, "Yolov7: Trainable bag-of-freebies sets new state-of-the-art for real-time object detectors," in *2023 IEEE/CVF Conference on Computer Vision and Pattern Recognition*, 2023, pp. 7464–7475.